Direct observation of a gap opening in topological interface states of MnSe/Bi2Se3 heterostructure

A. V. Matetskiy, I. A. Kibirev, T. Hirahara, S. Hasegawa, A. V. Zotov, and A. A. Saranin

---

Articles you may be interested in

Structural properties of Bi2− x Mn x Se3 thin films grown via molecular beam epitaxy
J. Appl. Phys. **118**, 045302 (2015); 10.1063/1.4927171

Epitaxial growth of the topological insulator Bi2Se3 on Si(111): Growth mode, lattice parameter, and strain state
Appl. Phys. Lett. **103**, 111909 (2013); 10.1063/1.4821181

Investigation of anomalous magnetoresistance in topological insulator Bi2Te3 at the onset of superconductivity in indium contacts
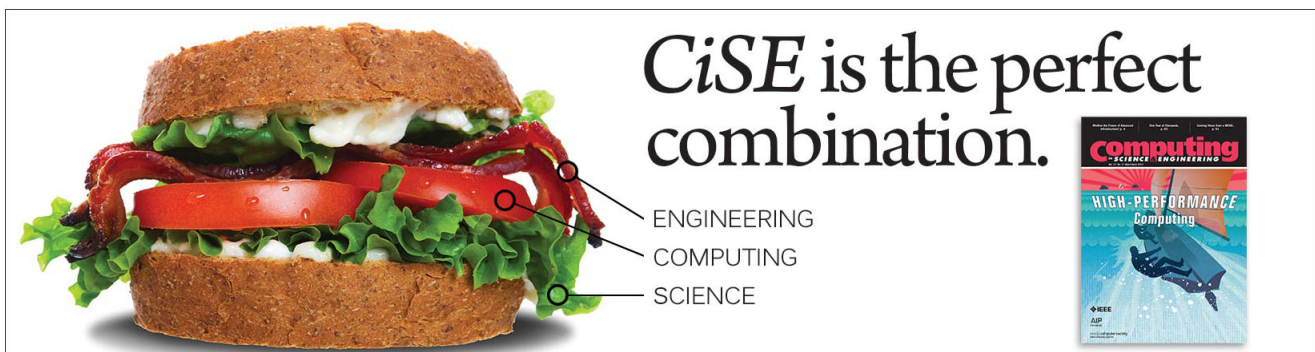J. Appl. Phys. **113**, 17C724 (2013); 10.1063/1.4798482

Enhanced contribution of surface state and modification of magnetoresistance in FexBi2−xSe3 topological insulator crystals
J. Appl. Phys. **113**, 043923 (2013); 10.1063/1.4790310

Epitaxial growth of Bi2Se3 topological insulator thin films on Si (111)
J. Appl. Phys. **109**, 103702 (2011); 10.1063/1.3585673

Direct observation of a gap opening in topological interface states of MnSe/Bi$_2$Se$_3$ heterostructure

A. V. Matetskiy,[1,2,a)] I. A. Kibirev,[1,2] T. Hirahara,[3] S. Hasegawa,[4] A. V. Zotov,[1,2,5] and A. A. Saranin[1,2]

[1]*Institute of Automation and Control Processes, Far Eastern Branch of RAS, Vladivostok 690041, Russian Federation*
[2]*Far Eastern Federal University, Vladivostok 690950, Russian Federation*
[3]*Department of Physics, Tokyo Institute of Technology, 2-12-1, Ookayama, Meguro-ku, Tokyo 152-8551, Japan*
[4]*Department of Physics, University of Tokyo, 7-3-1 Hongo, Bunkyo-ku, Tokyo 113-0033, Japan*
[5]*Department of Electronics, Vladivostok State University of Economics and Service, 690600 Vladivostok, Russian Federation*

High-quality MnSe(111) film was bilayer-by-bilayer grown epitaxially onto the Bi$_2$Se$_3$(111) surface using molecular beam epitaxy. Reversal scenario with quintuple layer-by-layer growth of Bi$_2$Se$_3$ onto the MnSe film was also realized. Angle-resolved photoemission spectroscopy measurements of Bi$_2$Se$_3$ capped with two bi-layers of MnSe revealed that an energy gap of about 90 meV appears at the Dirac point of the original Bi$_2$Se$_3$ surface, possibly due to breaking the time-reversal symmetry on the Bi$_2$Se$_3$ surface by magnetic proximity effect from MnSe. © 2015 AIP Publishing LLC.
[http://dx.doi.org/10.1063/1.4930151]

Unique quantum mechanical properties of topological insulators (TI) as well as their name originate from nontrivial topology in Hilbert space spanned by wave functions of their electronic states. At the interface of insulators with trivial and nontrivial topology, the energy gap has to be closed for the sake of changing topology. As a result, gapless surface states with Dirac-cone dispersion are formed. In the time-reversal invariant systems, the nontrivial topology of TIs is protected by time-reversal symmetry (TRS). At the same time, robustness of the topological surface states against non-magnetic perturbation and disorder is also associated with TRS.[1–3]

On the other hand, violation of TRS in such systems will lead to another set of fascinating effects. Exchange field would lift the Kramers degeneracy at the Dirac point and introduce a mass into the Dirac equation, that is, the critical point for observation of quantum anomalous Hall effect (QAHE) and topological magnetoelectric effect (TME).[1] There are two common ways to introduce ferromagnetic order into the system for violating TRS: doping by magnetic atoms during the crystal growth and magnetic proximity effect at the surface. Both of them have their strengths and weaknesses.[4]

Doping is a convenient method and shows some remarkable results. For the Te-based TIs, ferromagnetic ordering was observed,[5,6] as well as QAHE.[7] However, these samples did not show a Zeeman gap at the topological surface states in the angle-resolved photoemission spectra (ARPES).[5] In contrast, a magnetically doped Bi$_2$Se$_3$ showed a gap up to several tens meV,[8] but very small or even no magnetic hysteresis in the transport and magnetic measurements.[5] In addition, the doping is not very useful for observing TME, because in order to reach the goal, the TRS should be broken

on the surface, but not in the bulk.[3] Proximity-induced magnetic field on the TIs can be obtained by depositing ferromagnetic metals on the surface of TIs,[9,10] albeit with a variable success.[11] Furthermore, such a continuous metallic layer will hide signal from TI.[4] Instead, several ferromagnetic insulators (FMI) such as EuS and MnSe were proposed as promising candidates for this purpose.[12,13] Experimentally, the proximity-induced interfacial magnetization of Bi$_2$Se$_3$ was realized in the systems with EuS,[14] Y$_3$Fe$_5$O$_{12}$,[15] and BaFe$_{12}$O$_{19}$ (Ref. 16) used as magnetic insulators.

In the present paper, we report experimental results on the growth of the antiferromagnetic MnSe film (ferromagnetic ordering in each (111) atomic plane with alternating spin directions from plane to plane[13]) on the Bi$_2$Se$_3$(111) and effect of such a coating on the topological surface states.

Thin-film growth using molecular beam epitaxy was conducted in a ultrahigh vacuum (UHV) chamber with a base pressure less than 5.0×10^{-10} Torr, equipped with reflection-high-energy electron diffraction (RHEED) facility. We used n-type Si(111) wafers (40–70 Ω cm) as substrates. Atomically clean Si(111)7 × 7 surface was prepared in situ by flashing to 1280 °C after the wafer was first outgassed at 600 °C for 6 h. Manganese, bismuth and selenium were evaporated from effusion cells with integrated shutters. The prepared samples were transferred into another UHV chamber, equipped with scanning tunneling microscopy (STM) and ARPES facilities, using evacuated transfer unit. ARPES measurements were conducted using VG Scienta R3000 electron analyzer and high-flux He discharge lamp ($h\nu = 21.2$ eV).

To prepare Bi$_2$Se$_3$, we used combination of the two well-known approaches.[17–19] First, we obtained a surface without dangling bonds by preparing Si(111)$\beta - \sqrt{3} \times \sqrt{3}$–Bi (Ref. 20) reconstruction. Then, three quintuple layers (QL) of Bi$_2$Se$_3$ were grown at relatively low sample temperature of about 150 °C to avoid reaction with the silicon substrate. At

a)mateckij@iacp.dvo.ru

this temperature, the film growth proceeds in QL-by-QL fashion in which RHEED specular-spot intensity oscillation was observed (Fig. 1(a)). To improve the crystal quality of the film, the other layers were grown at a higher temperature of about 240 °C at which the film grew in step-flow mode. To reduce the amount of Se vacancies, the Bi-to-Se flux ratio was chosen close to 1:14 (Ref. 19) with the growth rate of about 0.3 QL/min.

MnSe has a rocksalt crystal structure with lattice constant in the (111) plane a = 3.86 Å (Ref. 21) which matches with that of Si(111) and is close to Bi_2Se_3 one. Direct overgrowth of MnSe on the Si substrate is not possible due to the formation of silicide. But, on the Bi_2Se_3 surface, the MnSe was easily grown epitaxially. We used the same Se-rich condition as for the MnSe growth, with the Mn rate being about 0.8 ML/min (monolayer, 7.8×10^{-14} cm^{-2}), at the sample temperature 240 °C. Under these conditions, RHEED specular-spot intensity oscillations corresponding to the bi-layer (BL)-by-BL growth, decreased rapidly (Fig. 1(b)), which indicated a transition to the step flow-growth mode. Reversal scenario of Bi_2Se_3 growth on top of the MnSe film was also realized using the same growth conditions (Fig. 1(c)), which opens a possibility of studying the interlayer exchange coupling in FMI/TI/FMI structure.[22]

The ratio of distances between streaks in the RHEED patterns (Fig. 1) for different top layers, Bi_2Se_3 ((a) and (c)) and MnSe (b) coincides well with the reciprocal ratio of lattice constants (Bi_2Se_3 –4.14 Å and MnSe –3.86 Å). The RHEED patterns indicated high crystal quality and absence

of any extrinsic spots. STM observations also confirmed high quality of the grown Bi_2Se_3 (Fig. 2(a)) and MnSe (Fig. 2(b)) films. The STM image, Fig. 2(d), of Bi_2Se_3 a half of which is covered by the bi-layer of MnSe was obtained by stopping the MnSe growth near the first minimum in the RHEED specular spot intensity plot in Fig. 1(b), showing that we obtained exactly the single-BL islands of MnSe. In the line profile of STM image in Fig. 2(d), one can see steps with two different heights of ≈0.9 nm and ≈0.3 nm, which correspond to the Bi_2Se_3 quintuple layer and MnSe bi-layer with 1 nm and 0.315 nm thick, respectively. For clarity, the crystal structures are given in Fig. 2(c).

Finally, we investigated the electronic structure of the grown films. Limited by electron escape depth,[23] we could only probe the buried topological interface states for the samples with small MnSe thicknesses of below 3 BL. Figure 3 shows ARPES band dispersion of the pristine Bi_2Se_3 (a) and that capped by 2 BL MnSe (b). Since possible slight tilt of sample with respect to the horizontal slit in the energy analyzer, could vary a gap size, if any, we conducted ARPES measurements at Γ_1 point, where we were sure that the spectrum cut crossed the center of Brillouin zone. In the band dispersion of pristine Bi_2Se_3 (Fig. 3(a)), one can see the bulk bands and the topological surface states (TSS) with Dirac point at ≈0.34 eV. In the energy distribution curve (EDC) at Γ_1 (Fig. 3(a), bottom), there is a single-peak structure at the Dirac point. For fitting the spectrum, we used two Lorentzian peaks to take into account the bulk valence band
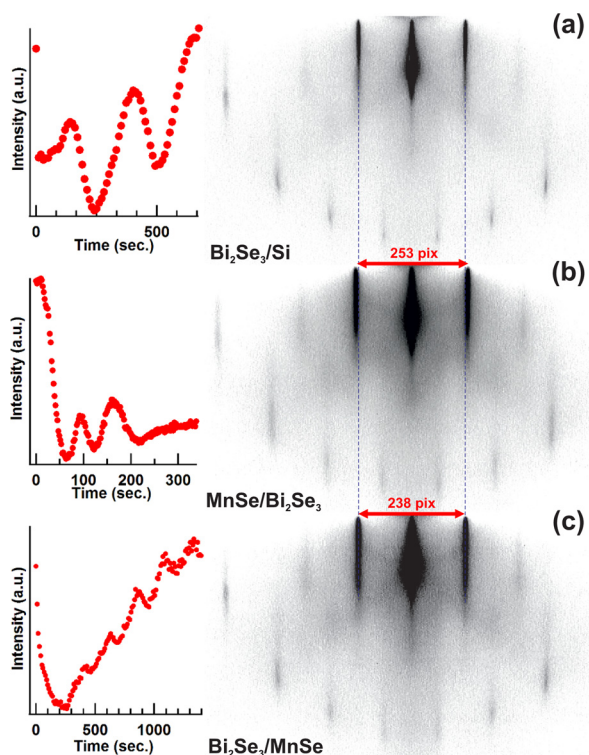

FIG. 1. Intensity oscillations of the RHEED specular spot during the initial stages of growth (left column) and corresponding RHEED patterns of the grown films (right column) of (a) 12 QL of Bi_2Se_3/Si(111), (b) 10 BL of MnSe/Bi_2Se_3/Si(111), and (c) 14 QL of Bi_2Se_3/MnSe/Bi_2Se_3/Si(111), respectively. The distance between streaks is marked by red arrows. Blue dotted lines are drawn through the centers of the Bi_2Se_3 RHEED streaks.
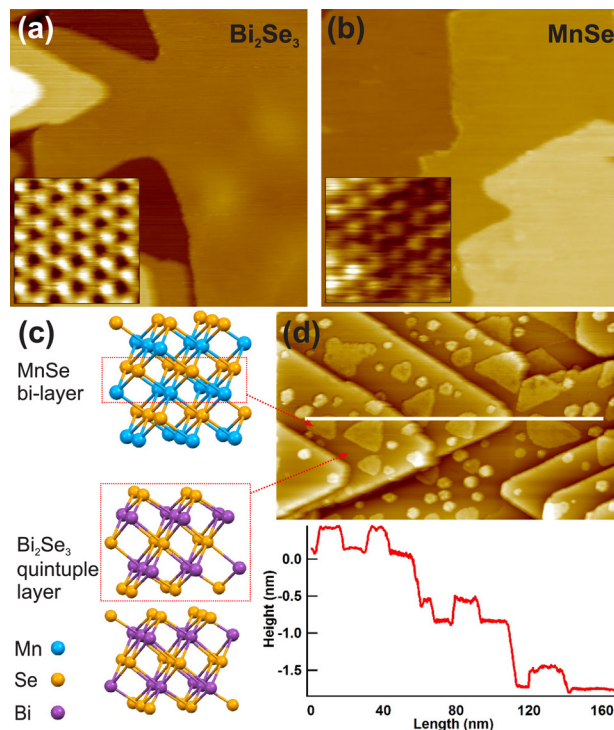

FIG. 2. STM images (200×200 nm^2, insets are 2×2 nm^2) of (a) 16 QL of Bi_2Se_3 film on Si(111) and (b) 2 BL of MnSe film grown on the Bi_2Se_3 film. (c) The crystal structures of MnSe and Bi_2Se_3. The dashed red frames mark the corresponding units of MnSe bi-layer and Bi_2Se_3 quintuple layer. (d) STM image (180×90 nm^2) of about a half of the bi-layer of MnSe grown on the Bi_2Se_3 film, and the corresponding STM height profile along a white line in the STM image. The line profile was acquired from the raw data, while the STM images were filtered using fast Fourier transform.
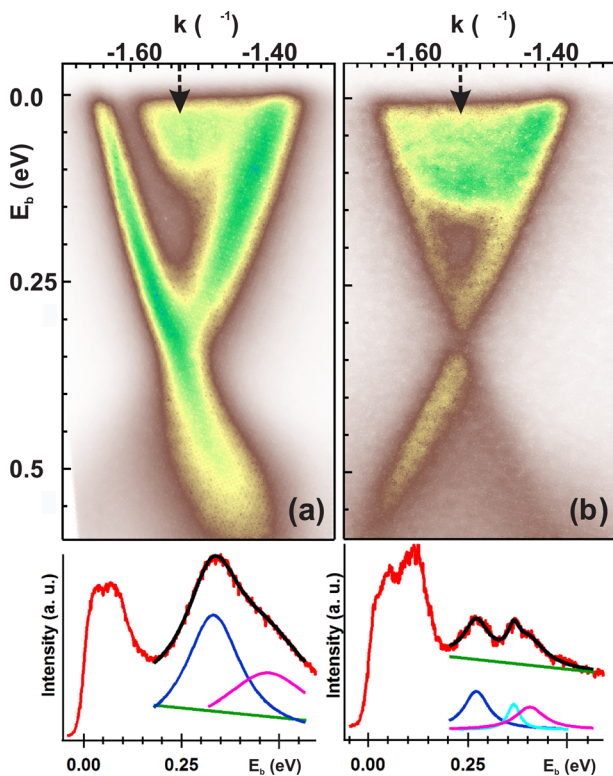
FIG. 3. Upper panel: ARPES band dispersion map around the Γ_1 point of (a) the initial 16 QL Bi_2Se_3 and (b) after overgrowth of 2 BL of MnSe on it. Lower panel: corresponding EDC curves taken at the center of Γ_1 point (marked by dark arrows). Fitting curves: green—linear background, blue and cyan—Lorentzian peaks of TSS and gapped TSS, pink—Lorentzian peak of the bulk valence band.

and Dirac cone.[24] In the band dispersion of Bi_2Se_3 with 2 BL of MnSe (Fig. 3(b)), one can clearly see a drop in intensity at the Dirac point. In the EDC, this corresponds to a double-peak structure. According to the fitting results, the gap size is about 90 meV—higher then those in the cases of Fe-doped[8] and Mn-doped[25] Bi_2Se_3 ($\leq$50 meV). Since we could not see clearly the gap opening at a 1 BL-MnSe covered Bi_2Se_3 (not shown here), the 2 BL of MnSe is believed to be a critical thickness for opening the gap.

However, other possible reasons for the loss of the spectral weight at the Dirac point cannot be excluded.[26] We can rule out the top-layer-relaxation caused by the mechanical cleavage[27] for our MBE grown samples. Then, according to Bergman and Refael[28] gap-like features can appear in case when continuum of bulk states overlaps with topological surface states. But in our case the bottom of conduction band moves to even higher binding energies. So, if the bulk band gap does not change, the top of the valence band would move even further from the Dirac point. Bulk band gap could vary due to possible manganese doping into the Bi_2Se_3, but according to Xu *et al.*[25] such intermixing would lead to a different bulk conduction band behavior. Anyway, we cannot exclude appearance of the impurities and defects states in Bi_2Se_3 after MnSe overgrowth, which might lead to broadening of the electronic states along momentum and energy axes and initiate the twin peak structure near the Dirac point.[27,29] Direct verification on the origin of the gap opening reported here could be gained with spin-resolved ARPES and anomalous Hall effect measurements.

In conclusion, epitaxial growth of a MnSe thin film on the Bi_2Se_3 (111) as well as the reversal growth of Bi_2Se_3 on MnSe were realized. It was shown that the films grew epitaxially with high crystallinity and sharp interfaces. Photoemission results unambiguously demonstrated that topological surface states at the interface of such a heterostructure remain, with developing an energy gap of about 90 meV at the Dirac point, possibly due to the broken time-reversal symmetry at the interface. Taking into account the high quality and straightforward and reliable preparation procedures, the grown heterostructures are believed to be convenient and promising candidates for observing quantum phenomena like topological magnetoelectric effect and quantum anomalous Hall effect.

[1] M. Z. Hasan and C. L. Kane, Rev. Mod. Phys. **82**, 3045 (2010).

[2] Y. Ando, J. Phys. Soc. Jpn. **82**, 102001 (2013).

[3] X. L. Qi and S. C. Zhang, Rev. Mod. Phys. **83**, 1057 (2011).

[4] C.-Z. Chang, P. Wei, and J. S. Moodera, MRS Bull. **39**, 867 (2014).

[5] J. Zhang, C.-Z. Chang, P. Tang, Z. Zhang, X. Feng, K. Li, L.-l. Wang, X. Chen, C. Liu, W. Duan, K. He, Q.-K. Xue, X. Ma, and Y. Wang, Science **339**, 1582 (2013).

[6] Y. S. Hor, P. Roushan, H. Beidenkopf, J. Seo, D. Qu, J. G. Checkelsky, L. a. Wray, D. Hsieh, Y. Xia, S. Y. Xu, D. Qian, M. Z. Hasan, N. P. Ong, a. Yazdani, and R. J. Cava, Phys. Rev. B **81**, 195203 (2010).

[7] C. Z. Chang, J. Zhang, X. Feng, J. Shen, Z. Zhang, M. Guo, K. Li, Y. Ou, P. Wei, L. L. Wang, Z. Q. Ji, Y. Feng, S. Ji, X. Chen, J. Jia, X. Dai, Z. Fang, S. C. Zhang, K. He, Y. Wang, L. Lu, X. C. Ma, and Q. K. Xue, Science **340**, 167 (2013).

[8] Y. L. Chen, J.-H. Chu, J. G. Analytis, Z. K. Liu, K. Igarashi, H.-H. Kuo, X. L. Qi, S. K. Mo, R. G. Moore, D. H. Lu, M. Hashimoto, T. Sasagawa, S. C. Zhang, I. R. Fisher, Z. Hussain, and Z. X. Shen, Science **329**, 659 (2010).

[9] Q. Liu, C. X. Liu, C. Xu, X. L. Qi, and S. C. Zhang, Phys. Rev. Lett. **102**, 156603 (2009).

[10] I. Vobornik, U. Manju, J. Fujii, F. Borgatti, P. Torelli, D. Krizmancic, Y. S. Hor, R. J. Cava, and G. Panaccione, Nano Lett. **11**, 4079 (2011).

[11] E. Wang, P. Tang, G. Wan, A. V. Fedorov, I. Miotkowski, Y. P. Chen, W. Duan, and S. Zhou, Nano Lett. **15**, 2031 (2015).

[12] S. V. Eremeev, V. N. Men'shov, V. V. Tugushev, P. M. Echenique, and E. V. Chulkov, Phys. Rev. B **88**, 144430 (2013).

[13] W. Luo and X.-L. Qi, Phys. Rev. B **87**, 085431 (2013).

[14] P. Wei, F. Katmis, B. a. Assaf, H. Steinberg, P. Jarillo-Herrero, D. Heiman, and J. S. Moodera, Phys. Rev. Lett. **110**, 186807 (2013).

[15] M. Lang, M. Montazeri, M. C. Onbasli, X. Kou, Y. Fan, P. Upadhyaya, K. Yao, F. Liu, Y. Jiang, W. Jiang, K. L. Wong, G. Yu, J. Tang, T. Nie, L. He, R. N. Schwartz, Y. Wang, C. a. Ross, and K. L. Wang, Nano Lett. **14**, 3459 (2014).

[16] W. Yang, S. Yang, Q. Zhang, Y. Xu, S. Shen, J. Liao, J. Teng, C. Nan, L. Gu, Y. Sun, K. Wu, and Y. Li, Appl. Phys. Lett. **105**, 092411 (2014).

[17] N. Bansal, Y. S. Kim, E. Edrey, M. Brahlek, Y. Horibe, K. Iida, M. Tanimura, G.-H. Li, T. Feng, H.-D. Lee, T. Gustafsson, E. Andrei, and S. Oh, Thin Solid Films **520**, 224 (2011).

[18] L. He, F. Xiu, Y. Wang, A. V. Fedorov, G. Huang, X. Kou, M. Lang, W. P. Beyermann, J. Zou, and K. L. Wang, J. Appl. Phys. **109**, 103702 (2011).

[19] H. D. Li, Z. Y. Wang, X. Kan, X. Guo, H. T. He, Z. Wang, J. N. Wang, T. L. Wong, N. Wang, and M. H. Xie, New J. Phys. **12**, 103038 (2010).

[20]R. H. Miwa, T. M. Schmidt, and G. P. Srivastava, J. Phys.: Condens. Matter **15**, 2441 (2003).
[21]A. J. Jacobson and B. E. F. Fender, J. Chem. Phys. **52**, 4563 (1970).
[22]M. Li, W. Cui, J. Yu, Z. Dai, Z. Wang, F. Katmis, W. Guo, and J. Moodera, Phys. Rev. B **91**, 014427 (2015).
[23]S. Hufner, *Photoelectron Spectroscopy* (Springer, Berlin/Heidelberg, 1996).
[24]Y. Xia, D. Qian, D. Hsieh, L. Wray, a. Pal, H. Lin, a. Bansil, D. Grauer, Y. S. Hor, R. J. Cava, and M. Z. Hasan, Nature Phys. **5**, 398 (2009).
[25]S.-Y. Xu, M. Neupane, C. Liu, D. Zhang, A. Richardella, L. Andrew Wray, N. Alidoust, M. Leandersson, T. Balasubramanian, J. Sánchez-Barriga, O. Rader, G. Landolt, B. Slomski, J. Hugo Dil, J. Osterwalder, T.-R. Chang, H.-T. Jeng, H. Lin, A. Bansil, N. Samarth, and M. Zahid Hasan, Nature Phys. **8**, 616 (2012).
[26]T. Sato, K. Segawa, K. Kosaka, S. Souma, K. Nakayama, K. Eto, T. Minami, Y. Ando, and T. Takahashi, Nature Phys. **7**, 840 (2011).
[27]S.-Y. Xu, L. a. Wray, N. Alidoust, Y. Xia, M. Neupane, C. Liu, H. W. Ji, S. Jia, R. J. Cava, and M. Z. Hasan, e-print arXiv:1206.0278.
[28]D. L. Bergman and G. Refael, Phys. Rev. B **82**, 195417 (2010).
[29]H. Beidenkopf, P. Roushan, J. Seo, L. Gorman, I. Drozdov, Y. S. Hor, R. J. Cava, and A. Yazdani, Nature Phys. **7**, 939 (2011).